

Experimental and Molecular Dynamics Simulation Study of the Sublimation Energetics of Cyclopentadienyltricarbonylmanganese (Cymantrene)

Ricardo Picciochi,^{†,‡} José N. Canongia Lopes,[‡] Hermínio P. Diogo,[‡] and Manuel E. Minas da Piedade^{*,†}

Departamento de Química e Bioquímica, Faculdade de Ciências, Universidade de Lisboa, 1649-016 Lisboa, Portugal, and Centro de Química Estrutural, Complexo Interdisciplinar, Instituto Superior Técnico, TULisboa, 1049-001 Lisboa, Portugal

Received: June 25, 2008; Revised Manuscript Received: July 31, 2008

The standard molar enthalpy of sublimation of monoclinic cyclopentadienyltricarbonylmanganese, $\text{Mn}(\eta^5\text{-C}_5\text{H}_5)(\text{CO})_3$, at 298.15 K, was determined as $\Delta_{\text{sub}}H_{\text{m}}^0[\text{Mn}(\eta^5\text{-C}_5\text{H}_5)(\text{CO})_3] = 75.97 \pm 0.37 \text{ kJ}\cdot\text{mol}^{-1}$ from Knudsen effusion and Calvet-drop microcalorimetry measurements, thus considerably improving the very large inaccuracy ($> 10 \text{ kJ}\cdot\text{mol}^{-1}$) of the published data. The obtained value was used to assess the extension of the OPLS-based all-atom force field we previously developed for iron metallocenes to manganese organometallic compounds. The modified force field was able to reproduce the volumetric properties (density and unit-cell volume) of crystalline $\text{Mn}(\eta^5\text{-C}_5\text{H}_5)(\text{CO})_3$ with a deviation of 0.6% and the experimentally determined enthalpy of sublimation with an accuracy of $1 \text{ kJ}\cdot\text{mol}^{-1}$. The interaction (ϵ) and atomic-diameter (σ) parameters of the Lennard-Jones (12-6) potential function used to calculate dispersion contributions within the framework of the force field were found to be transferable from iron to manganese.

Introduction

In previous publications, we have introduced a new all-atom force field for metallocenes to be used within the framework of statistical mechanics.^{1,2} The force field was initially developed by using quantum chemistry and molecular dynamics (MD) calculations and validated by comparing the simulation results with structural data for different ferrocene derivatives from single-crystal X-ray diffraction experiments.¹ It was later tested and refined against experimentally determined sublimation and vaporization enthalpies for some of those and a few other members of the ferrocene family.² Particular care was taken in the characterization of the solid samples in terms of chemical purity and phase purity, so that the $\Delta_{\text{sub}}H_{\text{m}}^0$ values used as benchmarks for the calculations could be assigned to specific crystal structures. The first effort toward a generalization of that force field to organometallic compounds of transition metals other than iron is described in this work and involves the study of cyclopentadienyltricarbonylmanganese (cymantrene), $\text{Mn}(\eta^5\text{-C}_5\text{H}_5)(\text{CO})_3$. Another objective was to resolve the large and long standing inaccuracy of the enthalpy of sublimation of $\text{Mn}(\eta^5\text{-C}_5\text{H}_5)(\text{CO})_3$: two $\Delta_{\text{sub}}H_{\text{m}}^0[\text{Mn}(\eta^5\text{-C}_5\text{H}_5)(\text{CO})_3]$ values at 298.15 K that differ by $\sim 12 \text{ kJ}\cdot\text{mol}^{-1}$ can be derived from previously reported vapor-pressure measurements^{3,4} (see below), and it had already been claimed that one of these data sets³ leads to a $\Delta_{\text{sub}}H_{\text{m}}^0[\text{Mn}(\eta^5\text{-C}_5\text{H}_5)(\text{CO})_3]$ value that seems impossibly low when compared with $\Delta_{\text{sub}}H_{\text{m}}^0[\text{Cr}(\eta^6\text{-C}_6\text{H}_6)(\text{CO})_3]$.⁵

The same strategy adopted before was followed in the expansion of the force field. Because the starting point of the simulations is the crystal structure of the compound of interest, instead of using a set of published enthalpy of sublimation data, which could not be ascribed to definite crystal structures, the development and validation steps were based on a single

compound, the enthalpy of sublimation of which was obtained by two independent experimental techniques, by using a well-characterized sample in terms of chemical and phase purity. From an experimental point of view, $\text{Mn}(\eta^5\text{-C}_5\text{H}_5)(\text{CO})_3$ offers the advantage of being easier to handle in air than $\text{Mn}(\eta^5\text{-C}_5\text{H}_5)_2$, which is the analogous of the ferrocene derivatives used in our previous studies.

It must be stressed that transition metals are already present in some other force fields, including extensions of the OPLS-AA/AMBER databases, from which the present model borrows part of the nonbonded interaction parameters of the Lennard-Jones potential function.^{6–9} In most cases, however, those force fields were designed to model large molecules of biological interest (e.g., proteins), where the intermolecular interactions are essentially controlled by the bulky organic backbones. This is probably at the heart of the apparent lack of physical meaning of the corresponding Lennard-Jones parameters obtained from MD simulations and crystal structure information. The atomic-diameter parameter, σ , for most transition-metal cations is smaller than that used for hydrogen (250 pm), and the interaction parameter, ϵ , can differ by as much as two orders of magnitude between neighboring transition metals (for instance Fe^{2+} , Cu^{2+} , and Zn^{2+}).⁹ This seems to have a negligible effect on the accuracy of the MD predictions for the properties of very large biomolecules, simply because the contribution of the metal is overshadowed by that of the organic residues. Even the energy involved in the docking of a substrate molecule to a metallic center is apparently not controlled by the size or dispersion forces related with the metal itself but by the complex structure and interactions of the large organic framework surrounding it.

A quite different situation is found, however, for small organometallic compounds, such as cyclopentadienyl derivatives, where the obtained MD results are much more sensitive to the contribution of the metal for the intermolecular interactions. To test just how sensitive they are to the nature of the metal, the transferability of the Lennard-Jones parameters

* Corresponding author. E-mail: memp@fc.ul.pt.

[†] Universidade de Lisboa.

[‡] Instituto Superior Técnico.

obtained for iron in our previous study of ferrocene derivatives to its close neighbor manganese was also investigated in this work.

Materials and Methods

General. The elemental analysis was carried out on a Fisons Instruments EA1108 apparatus. The IR spectrum was recorded in a Jasco FT/IR 4100 spectrophotometer calibrated with polystyrene film, using KBr, plates. The ^1H NMR and ^{13}C NMR spectra were obtained at ambient temperature on a Bruker Ultrashield 300 MHz spectrometer. X-ray powder diffractometry (XRD) experiments were performed at 293 ± 2 K over the range $13 \leq 2\theta \leq 43^\circ$ on a D8 Bruker AXS Advanced diffractometer, by employing Cu K α radiation ($\lambda = 1.54178$ Å). The scan speed was $0.5^\circ (2\theta \cdot \text{min}^{-1})$ with a step size $0.020^\circ (2\theta)$. The indexation of the powder pattern was performed by using the program Checkcell.¹⁰ The temperature and enthalpy of fusion measurements were made with a 2920 MTDSC temperature-modulated differential scanning calorimeter (DSC) from TA Instruments operated as a conventional DSC. The temperature and heat flow scales of the instrument were calibrated as previously described.¹¹ The samples were sealed under air in aluminum pans and weighed to ± 0.1 μg on a Mettler UMT2 ultramicro balance. Helium (Air Liquide N55) at a flow rate of $30 \text{ cm}^3 \cdot \text{min}^{-1}$ was used as the purging gas.

Mn($\eta^5\text{-C}_5\text{H}_5$)(CO) $_3$. Cyclopentadienyltricarbonylmanganese ([CAS 12079-65-1], Aldrich 98%) was purified by sublimation at 298 K and 0.13 Pa prior to use. Elemental analysis for $\text{C}_8\text{H}_5\text{O}_3\text{Mn}$: Expected C 47.09%, H 2.47%; found C 47.04%, H 2.33% (average of two determinations). FT-IR (KBr, main peaks): $\tilde{\nu}/\text{cm}^{-1} = 3128$ (CH stretch, ν_1); 2017 (CO stretch); 1911 (CH stretch); 1421 (CC stretch, ν_8); 1059 (CH bend, e_2); 1012 (CH bend, ν_6); 939 (ring distortion, ν_{13}); 846–834 (CH bend, ν_7 and ν_2); 667 (Mn–C–O bend, a_1); 633 (Mn–C–O bend, e); 542 (Mn–C–O bend, e). The assignments were based on literature data.^{12,13} ^1H NMR (400 MHz, CDCl_3/TMS): $\delta = 4.756$ (s, 5H, C_5H_5); ^{13}C NMR (400 MHz, CDCl_3/TMS): $\delta = 82.79$ (s, 5C, C_5H_5), $\delta = 224.1$ (s, 3C, CO). The results of the ^{13}C NMR spectra are in good agreement with the previously reported values $\delta = 83.1$ and $\delta = 225.1$.^{14,15} The powder pattern was indexed as monoclinic, space group $P2_1/a$, with $a = 11.99$ Å, $b = 7.07$ Å, $c = 10.93$ Å, and $\beta = 117.8^\circ$. These values are in good agreement with $a = 12.077(3)$ Å, $b = 7.057(2)$ Å, $c = 10.913(2)$ Å, and $\beta = 117.68(2)^\circ$, previously obtained at room temperature from single-crystal X-ray diffraction experiments.^{16,17} No phase transitions other than fusion were detected by DSC in the range between 283 K and the fusion temperature when using samples with masses in the range of 3.9–6.3 mg and a scan rate of $3 \text{ K} \cdot \text{min}^{-1}$. The onset (T_{on}) and the maximum (T_{max}) temperatures of the fusion peak were $T_{\text{on}} = 349.34 \pm 0.12$ K and $T_{\text{max}} = 350.13 \pm 0.09$ K. The corresponding enthalpy of fusion was $\Delta_{\text{fus}}H_{\text{m}}^0 = 18.9 \pm 0.3 \text{ kJ} \cdot \text{mol}^{-1}$. The uncertainties quoted are twice the standard deviation of the mean of four independent determinations. These results are in good agreement with the previously reported $T_{\text{fus}} = 350$ K and $\Delta_{\text{fus}}H_{\text{m}}^0 = 19.3 \text{ kJ} \pm 0.4 \text{ kJ} \cdot \text{mol}^{-1}$.⁵

Heat Capacity Measurements. The heat capacity (here taken as $C_{p,m}^0$) of solid cyclopentadienyltricarbonylmanganese in the range 280–318 K was determined with a Setaram DSC 121 apparatus by using a reported method.¹⁸ Two independent runs were carried out at a heating rate of $1 \text{ K} \cdot \text{min}^{-1}$. The samples, with masses of 286.08 and 289.39 mg, were enclosed in aluminum pans. Argon (Air Liquide N55) at a flow rate of 17

$\text{cm}^3 \cdot \text{min}^{-1}$ was used as the purging gas. Synthetic sapphire ($\alpha\text{-Al}_2\text{O}_3$ pellets, NIST-RM 720) was used as heat capacity standard.

Enthalpy of Sublimation Measurements. The enthalpy of sublimation of $\text{Mn}(\eta^5\text{-C}_5\text{H}_5)(\text{CO})_3$ was determined by Knudsen effusion and Calvet-drop microcalorimetry. The Knudsen effusion apparatus and operating procedure have been previously described.^{19–21} The thickness, radius, and area of the effusion hole, made in a copper foil (Cu 99%, Goodfellow Metals) and soldered to the cell lid, were $l = 2.090 \times 10^{-5}$ m, $r = 2.588 \times 10^{-4}$ m, and $A = 2.105 \times 10^{-7}$ m 2 . The cell was inserted in a brass block at the bottom of the vacuum chamber. This block was immersed in a water bath, the temperature of which was controlled to 0.01 K with a Haake ED Unitherm thermostat and a Haake EK12 cryostat as the heat sink. The temperature inside the cell was assumed to be equal to the temperature of the brass block. It was measured with a precision of ± 0.1 K by a Tecnisis 100 Ω platinum resistance thermometer embedded in the block and connected in a four-wire configuration to a Keithley 2000 multimeter. The cell was initially charged with ca. 160 mg of sample, and the mass loss in each run was determined to ± 0.01 mg with a Mettler AT201 balance.

The Calvet microcalorimetry experiments were carried out on an electrically calibrated drop-sublimation apparatus.^{22,23} In a typical experiment, the sample with a mass in the range 4.7–13.2 mg was placed into a small glass capillary and weighed with a precision of 1 μg in a Mettler M5 microbalance. The capillary was equilibrated for ca. 15 min at 298 K, inside a furnace placed above the entrance of the calorimetric cell, and subsequently dropped into the cell under N_2 atmosphere. The temperature of the calorimetric cell was set to 305.15 K. After dropping, an endothermic peak due to the heating of the sample from room temperature to the temperature of the calorimeter was first observed. When the signal returned to the baseline, the sample and reference cells were simultaneously evacuated to 0.13 Pa, and the measuring curve corresponding to the sublimation of the compound was acquired. The corresponding enthalpy of sublimation was derived from the area of the obtained curve and the calibration constant of the apparatus. No decomposition residues were found inside the calorimetric cell at the end of the experiments.

Density Functional Theory Calculations. Density functional theory (DFT) calculations were carried out with the Gaussian-03 program.²⁴ Full geometry optimizations and frequency predictions were carried out by using the Becke's three-parameter hybrid method²⁵ with the Perdew and Wang PW91²⁶ correlation functional (B3PW91) and the SDDall basis set (SDD effective core potentials and triple- ζ valence basis sets on all heavy atoms and D95 for hydrogens).^{27,28} In previous tests, the B3PW91/SDDall model proved to be a reliable, economical, and practical approach to obtain accurate geometrical data for ferrocene derivatives.¹ Atomic point charges (ESP charges) were determined at the B3PW91/6-311G(3df,3pd) level of theory, through a fit to the molecular electrostatic potential, by using the CHelpG procedure²⁹ and the B3PW91/SDDall equilibrium geometry.

MD Simulations. The MD runs on $\text{Mn}(\eta^5\text{-C}_5\text{H}_5)(\text{CO})_3$ were performed by using the DL_POLY package³⁰ and a refined version² of the previously reported all-atom force field¹ developed for ferrocene and its derivatives within the framework of the OPLS-AA parametrization. New terms associated with the three carbonyl groups bonded to the manganese atom had to be obtained. The complete set of parameters used in the simulations is indicated in Table 1, where q refers to the atomic

TABLE 1: Force-Field Parameters for Mn(η^5 -C₅H₅)(CO)₃

atoms	$q/a.c.u$	$\epsilon/kJ \cdot mol^{-1}$	$\sigma/\text{\AA}$
Mn	-0.11	1.200	3.11
C _{CO}	+0.21	0.440	3.75
O _{CO}	-0.18	0.879	2.96
C _{Cp}	-0.07	0.293	3.55
H _{Cp}	+0.11	0.126	2.42
bonds	$k_r/kJ \cdot mol^{-1} \cdot \text{\AA}^{-2}$	$r_o/\text{\AA}$	$r_{o,XRD}/\text{\AA}^a$
Mn-C _{Cp}	rigid	2.13	2.124 ± 0.005
Mn-C _{CO}	1686	1.78	1.780 ± 0.007
C _{Cp} -C _{Cp}	rigid	1.43	1.39 ± 0.02
C _{Cp} -H _{Cp}	rigid	1.08	0.93 ± 0.04
C _{CO} -O _{CO}	9618	1.19	1.150 ± 0.007
angles	$k_\theta/kJ \cdot mol^{-1} \cdot rad^{-2}$	θ_o/deg	$\theta_{o,XRD}/^\circ{}^b$
C _{Cp} -C _{Cp} -H _{Cp}	293	126	126
Mn-C _{CO} -O _{CO}	rigid	180	178.9
C _{CO} -Mn-C _{CO}	295	93	92
X _{Cp} -Mn-C _{CO} ^b	205	124	

^a References 16 and 17. ^b X_{Cp} refers to the centroid of the cyclopentadienyl ring.

point charges, ϵ is the interaction parameter, and σ is the atomic-diameter parameter of the Lennard-Jones (12-6) potential function, r_o and θ_o refer to the equilibrium bond distances and angles, respectively, and k_r and k_θ denote bond stretching and angle bending force constants, respectively. The numbers in normal typeface were taken directly from the OPLS-AA force field or adapted from the previously used parametrization for ferrocene derivatives;^{1,2} those in bold are the result of quantum chemical calculations performed in the present study.

The atomic point charges were calculated from the electron density obtained at the B3PW91/6-311G(3df,3pd) level of theory by using the electrostatic surface potential methodology described above. The ϵ and σ terms for each type of nonmetallic atom present in the Mn(η^5 -C₅H₅)(CO)₃ molecule were taken from the OPLS-AA model. The corresponding parameters for manganese were assumed to be identical to those previously recommended for iron.² This approximation was used to test the transferability of force-field parameters between different first-row transition metals, which is one of the objectives of the present work. In cases where direct transfer from the OPLS-AA force field was not possible, the equilibrium distances and angles were estimated by using the B3PW91/SDDall model. For comparison, the corresponding data from X-ray diffraction experiments are also included in Table 1 ($r_{o,XRD}$ and $\theta_{o,XRD}$).^{16,17} Stretching and bending force constants were also directly taken from the OPLS-AA force field or estimated from normal-mode frequencies calculated by the B3PW91/SDDall model, without scaling. Whenever necessary, the correlation by Halgren³¹ was used to obtain the corresponding angle-bending force constants from the calculated normal-mode frequencies.

It should be noted that the present force-field model is designed to study equilibrium thermodynamic properties in condensed phases, which are not very sensitive to some intramolecular features that have fast time scales, such as bond stretching and angle bending. Generally, within this scope, the parameters for stretching and bending force constants are easier to transfer than those for equilibrium distances and angles. The last two affect the geometry and conformations of the molecules which normally have a significant impact on the crystal packing, thus affecting the prediction of volumetric (e.g., density, unit-cell volume) and energetic (e.g., enthalpy of sublimation) properties.

As in the case of ferrocene derivatives, the carbon atom framework of the cyclopentadienyl ring was modeled as a rigid regular pentagon positioned at a fixed distance from the metallic center. The Mn-C-O angles were fixed at 180° to avoid divergence problems. All other bonds and angles were modeled by using the harmonic potentials used in the OPLS-AA force field. The parameters corresponding to the C_{Cp}-Mn-C_{CO}-O_{CO} dihedrals were all set to zero, because a potential energy scan performed at the B3PW91/SDDall level of theory led to the conclusion that the barrier for the internal rotation of the Cp ring amounts to only 0.15 kJ·mol⁻¹, so that the torsion energy profile of the molecule can be mainly attributed to nonbonded (stereochemical hindrance) effects.

The condensed phases were modeled as boxes containing a 180 molecules of Mn(η^5 -C₅H₅)(CO)₃, which correspond to 3000 atoms and to cutoff distances of 1.4 nm. The Ewald summation technique was used to account for long-range interactions beyond those cutoffs. The simulation boxes and initial configurations were set by taking into account the dimensions and occupancy of the unit cell of the published experimental crystalline structure.^{16,17} Because the unit-cell dimensions of the crystals were too small to accommodate a sufficiently large cutoff distance, well-proportioned simulation boxes consisting of several stacked cells were used. The simulations were performed at 298 K and 0.1 MPa, under the anisotropic isothermal-isobaric ensemble (*NσT*). Typical runs consisted of an equilibration period of ca. 100 ps followed by production stages of 400 ps. Other details concerning the simulation of crystalline structures obtained by using an OPLS-based force field can be found elsewhere.^{1,32} The vapor phase was also modeled at 298 K and 0.1 MPa, via isolated molecules in the canonical (*NVT*) ensemble. Because the statistics are poor due to the small number of atoms, each production run took 40 ns, and 20 such runs were used to calculate the average gas-phase properties.

Results and Discussion

The 2005 IUPAC recommended standard atomic masses were used in the calculation of all molar quantities.³³

Knudsen Effusion and Calvet-Drop Microcalorimetry Experiments. The vapor pressures, p , of Mn(η^5 -C₅H₅)(CO)₃ obtained in the Knudsen effusion experiments were calculated from^{34,35}

$$p = \frac{m}{At} \left(\frac{2\pi RT}{M} \right)^{1/2} \left(\frac{8r + 3l}{8r} \right) \left(\frac{2\lambda}{2\lambda + 0.48r} \right) \quad (1)$$

where m is the mass loss during the time t ; A , l , and r are the area, the thickness, and the radius of the effusion hole, respectively, M is the molar mass of the compound under study, R is the gas constant, T is the absolute temperature, and λ is the mean free path given by³⁶

$$\lambda = \frac{kT}{\sqrt{2}\sigma^2 p} \quad (2)$$

Here, k represents the Boltzmann constant, and σ represents the collision diameter. The collision diameter of Mn(η^5 -C₅H₅)(CO)₃ was estimated as 645 pm from the van der Waals volume of the molecule calculated with the GEPOL93 program³⁷ based on the molecular structure reported by Fitzpatrick et al.^{16,17} The van der Waals radii of carbon (1.70 Å), hydrogen (1.20 Å), and oxygen (1.52 Å) given by Bondi³⁸ and that recommended for manganese (2.00 Å) in the Cambridge Structural Database¹⁷ were selected for this calculation. Because the mean free path in eq 2 is pressure-dependent, an iterative method was

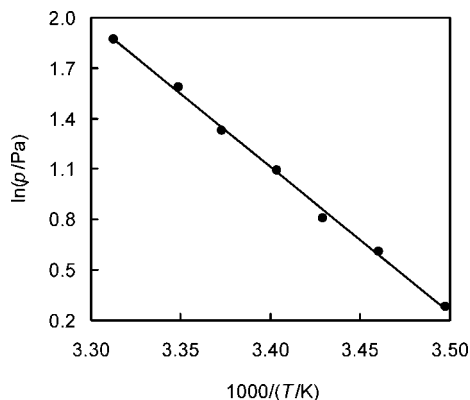


Figure 1. Vapor pressures of $\text{Mn}(\eta^5\text{-C}_5\text{H}_5)(\text{CO})_3$ as a function of the temperature obtained in the Knudsen experiments.

needed to obtain the vapor pressure of the compound through eqs 1 and 2. As a first approximation, p was calculated by ignoring the λ -dependent term in eq 1. The obtained result was subsequently used to derive λ from eq 2. The calculated mean free path was introduced in eq 1, and a second p value was calculated. The iteration was continued until the difference between successive values of p was smaller than 10^{-8} Pa. The vapor pressure against temperature data (see Supporting Information for details) were fitted to eq 3 (Figure 1)³⁹

$$\ln p = a + \frac{b}{T} \quad (3)$$

where the slope b is related to the enthalpy of sublimation at the average of the highest and lowest temperatures of the range covered in each series of experiments, $T_m = 293.9$ K, by $\Delta_{\text{sub}}H_m^0(T_m) = -bR$. The obtained results were $a = 30.62 \pm 0.65$, $b = -8678.5 \pm 190.3$, and $\Delta_{\text{sub}}H_m^0(293.9 \text{ K}) = 72.16 \pm 3.87 \text{ kJ}\cdot\text{mol}^{-1}$. The uncertainties quoted for a and b are the corresponding standard errors, and that for $\Delta_{\text{sub}}H_m^0(T_m)$ includes Student's factor for 95% confidence level ($t = 2.447$ for seven independent measurements).⁴⁰ The enthalpy of sublimation of $\text{Mn}(\eta^5\text{-C}_5\text{H}_5)(\text{CO})_3$ at 298.15 K, $\Delta_{\text{sub}}H_m^0[\text{Mn}(\eta^5\text{-C}_5\text{H}_5)(\text{CO})_3] = 72.02 \pm 3.87 \text{ kJ}\cdot\text{mol}^{-1}$, was computed from

$$\Delta_{\text{sub}}H_m^0(298.15 \text{ K}) = \Delta_{\text{sub}}H_m^0(T) + \int_T^{298.15 \text{ K}} [C_{p,m}^0(\text{g}) - C_{p,m}^0(\text{cr})] dT \quad (4)$$

where $C_{p,m}^0(\text{g})$ and $C_{p,m}^0(\text{cr})$ are the molar heat capacities of the compound in the gaseous and crystalline states, respectively. The calculation was based on the equations ($C_{p,m}^0$ in $\text{J}\cdot\text{mol}^{-1}\cdot\text{K}^{-1}$):

$$C_{p,m}^0(\text{g}) = 0.4559T + 43.276 \quad (5)$$

$$C_{p,m}^0(\text{cr}) = 0.4273T + 82.832 \quad (6)$$

Eq 5 was derived from a linear least-squares fitting to the $C_{p,m}^0(\text{g})$ values in the range 280–320 K, calculated by statistical thermodynamics,⁴¹ by using structural and unscaled vibration frequency data obtained at the B3PW91/SDDAll level of theory, together with harmonic-oscillator/rigid-rotor partition functions. Equation 6 was determined from a similar fitting to the $C_{p,m}^0(\text{cr})$ results obtained by DSC in the range 280–318 K. Where comparison is possible, these results agree to within 1–2% with the corresponding adiabatic calorimetry data reported for temperatures below 300 K.⁵

The enthalpy of sublimation of $\text{Mn}(\eta^5\text{-C}_5\text{H}_5)(\text{CO})_3$ was also measured by Calvet drop-sublimation microcalorimetry, at 305.2

K, leading to $\Delta_{\text{sub}}H_m^0(305.2 \text{ K}) = 75.80 \pm 0.37 \text{ kJ}\cdot\text{mol}^{-1}$. The uncertainty quoted represents twice the standard error of the mean of six independent results (detailed results are given as Supporting Information). Correction of this value to 298.15 K by using eqs 4–6 leads to $\Delta_{\text{sub}}H_m^0[\text{Mn}(\eta^5\text{-C}_5\text{H}_5)(\text{CO})_3] = 76.01 \pm 0.37 \text{ kJ}\cdot\text{mol}^{-1}$, in good agreement with the result of the Knudsen effusion experiments within their combined uncertainty intervals. The weighed mean⁴² of the values obtained by both techniques, $\Delta_{\text{sub}}H_m^0 = 75.97 \pm 0.37 \text{ kJ}\cdot\text{mol}^{-1}$, was selected in this work.

To the best of our knowledge only two studies leading to the enthalpy of sublimation of $\text{Mn}(\eta^5\text{-C}_5\text{H}_5)(\text{CO})_3$ have been published. From the vapor pressures obtained by Cordes and Schreiner,³ at three temperatures in the range 335.0–343.2 K, by using the Knudsen effusion method, it is possible to derive $\Delta_{\text{sub}}H_m^0(339.2 \text{ K}) = 64.2 \pm 11.6 \text{ kJ}\cdot\text{mol}^{-1}$. The indicated uncertainty includes Student's factor for 95% confidence level ($t = 4.303$).⁴⁰ On the other hand, the vapor pressures of $\text{Mn}(\eta^5\text{-C}_5\text{H}_5)(\text{CO})_3$ given by Baev and Demiyanchuk,⁴ in the range 323.2–353.2 K, lead to $\Delta_{\text{sub}}H_m^0(338.2 \text{ K}) = 52.7 \pm 3.1 \text{ kJ}\cdot\text{mol}^{-1}$, where the uncertainty quoted is that given by the authors. The correction of these two values to 298.15 K, by using equations 4–6, gives $\Delta_{\text{sub}}H_m^0 = 65.5 \pm 11.6 \text{ kJ}\cdot\text{mol}^{-1}$ and $\Delta_{\text{sub}}H_m^0 = 53.9 \pm 3.1 \text{ kJ}\cdot\text{mol}^{-1}$, respectively. In absolute terms, these two results differ by $10.5 \text{ kJ}\cdot\text{mol}^{-1}$ and $22.0 \text{ kJ}\cdot\text{mol}^{-1}$, respectively, from that recommended in this work ($75.97 \pm 0.37 \text{ kJ}\cdot\text{mol}^{-1}$), although agreement is observed with the value ensuing from the work of Cordes and Schreiner³ ($\Delta_{\text{sub}}H_m^0 = 65.5 \pm 11.6 \text{ kJ}\cdot\text{mol}^{-1}$) when its large uncertainty interval is taken into account. The origin of these discrepancies was impossible to ascertain. It is, however, unlikely that they result from the existence of phase transitions separating the temperature ranges of the present measurements and those of the previously reported data, as earlier found in the case of ferrocenecarboxaldehyde.² As mentioned in the Materials and Methods section, no phase transitions other than fusion were noticed during the DSC characterization of $\text{Mn}(\eta^5\text{-C}_5\text{H}_5)(\text{CO})_3$ in the range 280–358 K. This observation is also corroborated by published results of adiabatic calorimetry and differential thermal analysis experiments in the ranges 5–300 K and 100–360 K, respectively.⁵

MD Simulations. The simulation results are compared in Table 2 with the corresponding experimental data taken from the literature^{16,17} or obtained in this work from the enthalpy of sublimation measurements. The calculated and experimental crystal densities of $\text{Mn}(\eta^5\text{-C}_5\text{H}_5)(\text{CO})_3$ differ by less than 0.6%. The agreement is excellent, when considering that the calculations are purely predictive (all structure-dependent parameters used were either taken or adapted from the OPLS-AA force field or obtained from DFT calculations; none was adjusted to match experimental crystallographic data) and that the 0.6% deviation is considerably smaller than those usually obtained when comparing the performance of a force field against experimental density data for molecular compounds, both in the crystalline and liquid phases ($\sim 3\%$).^{6,7} The model was also able to accurately predict the structural properties of crystalline $\text{Mn}(\eta^5\text{-C}_5\text{H}_5)(\text{CO})_3$. In general, after relaxation, the experimental unit-cell dimensions and volume were reproduced with deviations of less than 2%. It must be noted that the MD data presented in Table 2 (cell parameters and unit-cell volume) are the mean values of the corresponding results obtained in all simulation runs. Any apparent inconsistency between the values of the cell parameters and the cell volume in that table is, therefore, due to this fact.

TABLE 2: Comparison of the MD Results with Experimental Data from XRD and Enthalpy of Sublimation Measurements at 298 K

unit cell	structure		energetics ^a			
	MD	XRD ^b				
<i>a</i> /Å	11.84 ± 0.03	12.077	$\Delta_{\text{sub}}U_{\text{conf,m}}^{\circ}$	tot	74.5 ± 0.6	(15.6; −58.9)
<i>b</i> /Å	7.21 ± 0.02	7.057		coul	9.4 ± 0.1	(−48.9; −58.3)
<i>c</i> /Å	11.05 ± 0.03	10.913		vdw	80.1 ± 0.9	(42.7; −37.4)
α /deg	90.00 ± 0.05	90		bnd	−2.8 ± 0.5	(6.7; 9.5)
β /deg	116.7 ± 0.1	117.68	$\Delta_{\text{sub}}H_{\text{m}}^{\circ}(\text{MD})$ $\Delta_{\text{sub}}H_{\text{m}}^{\circ}(\text{Exp})$	ang	−12.2 ± 0.8	(15.1; 27.3)
γ /deg	90.00 ± 0.05	90			77.0 ± 0.6	
<i>V</i> /Å ³	827.7 ± 0.3	823.644			75.97 ± 0.37 ^c	
ρ /g·cm ^{−3}	1.637	1.646				

^a All data in kJ·mol^{−1}. The values in parenthesis correspond to the molar configurational energies ($U_{\text{conf,m}}^{\circ}$) of the gaseous and crystalline states (gas; solid) obtained in the simulation runs. ^b References 16 and 17. ^c This work.

As mentioned above, the values of the ε and σ parameters for the manganese atom were assumed to be identical to those used for the iron atom in iron metallocene. Even with this approximation, the model was able to predict the experimentally determined standard molar enthalpy of sublimation of Mn(η^5 -C₅H₅)(CO)₃ at 298.15 K with a deviation smaller than 1.5%. This is in the lower limit of the errors found in the study of ferrocene derivatives without severe steric constraints (1.5–5.7%).² As previously noted, relative errors larger than those observed for the volumetric properties (0.6% in the case of the density and unit-cell volume) may be expected to occur for the prediction of $\Delta_{\text{sub}}H_{\text{m}}^{\circ}$.² The standard molar enthalpies of sublimation are calculated from

$$\Delta_{\text{sub}}H_{\text{m}}^{\circ} = U_{\text{conf,m}}^{\circ}(\text{g}) - U_{\text{conf,m}}^{\circ}(\text{cr}) + RT \quad (7)$$

where $U_{\text{conf,m}}^{\circ}$ represents the standard molar configurational internal energy. Thus, unlike the density and the unit-cell volume which are obtained from a single simulation run modeling the crystalline phase, the calculation of $\Delta_{\text{sub}}H_{\text{m}}^{\circ}$ involves the difference between two configurational-internal-energy values. These are obtained from two independent simulation runs, one referring to the condensed phase and another to the gas phase. The uncertainties associated with each run will add up in the calculation of the errors of the $U_{\text{conf,m}}^{\circ}(\text{g}) - U_{\text{conf,m}}^{\circ}(\text{cr})$ difference in eq 7. Thus, when both $U_{\text{conf,m}}^{\circ}$ contributions are large and have the same sign, their difference is smaller than each individual value, and a large relative error can be obtained. This is particularly important for simulations performed in the gas phase which refer to a single molecule. Although the simulation times are typically two orders of magnitude larger than those selected for the corresponding condensed-phase simulation runs, the variations associated with any given configuration lead to values with large uncertainty intervals. In summary, the agreement between the simulation and experimental $\Delta_{\text{sub}}H_{\text{m}}^{\circ}$ results in Table 2 can be considered excellent, given the purely predictive nature of the model and its reported performance in the case of iron metallocenes.

MD simulations also allow the calculation of different contributions to the molar configurational energy of a given system. The interactions associated with those contributions are normally subdivided into two groups: (i) the nonbonded interactions, which include those of Coulombic and van der Waals nature and (ii) the bonded interactions involving bonds, angles, and dihedrals. Although group (i) is generally associated with intermolecular interactions (which are prevalent in the modeling of the sublimation process) and group (ii) is associated with intramolecular interactions (the contribution to a sublimation process of which generally cancels out), the frontier between both categories is not sharp, because there are also nonbonded

interactions that act at the intramolecular level. The individual contributions to the total (tot) conformational energies of Mn(η^5 -C₅H₅)(CO)₃ in the gaseous and crystalline phases (and their differences), due to Coulombic (coul), van der Waals (vdw), bond (bnd), and angle (ang) interactions, are also listed in Table 2. In this case, no dihedral contributions exist because, as mentioned above, all C_{CP}–Mn–C_{CO}–O_{CO} dihedrals were set to zero. The most prominent values correspond to the van der Waals terms, which show that the crystalline phase is ca. 80 kJ·mol^{−1} more stable than the gaseous phase because of the dispersion interactions. This overshoot relative to an experimental enthalpy of sublimation of 75.97 ± 0.37 kJ·mol^{−1} is compensated by a negative value of the angle interactions (the gas is 12 kJ·mol^{−1} more stable than the solid). The origin of this unexpectedly large angle contribution (bonded interactions should in principle cancel out, because they mainly reflect intramolecular interactions) may be related to the relaxation of the three C_{CO}–Mn–C_{CO} angles on going from the crystalline phase, where they can be distorted by the packing of the molecules, to the gas phase, where they may be closer to their energy minimum. If one envisages Mn(η^5 -C₅H₅)(CO)₃ as a three-legged stool, one can imagine that the angles between the three legs may be deformed if one sits on it. The two other contributions (from electrostatic and bond interactions) lead to a total sublimation enthalpy of 77 kJ·mol^{−1}, which, as mentioned above, is in good agreement with the corresponding experimental value. It is finally worth noticing that electrostatics play a relatively minor role in the sublimation of Mn(η^5 -C₅H₅)(CO)₃.

Acknowledgment. This work was supported by Fundação para a Ciência e a Tecnologia, Portugal (Project PPCDT/QUI/56880/2004).

Supporting Information Available: Table S1: powder pattern indexation for the Mn(η^5 -C₅H₅)(CO)₃ sample used in this work. Tables S2 and S3: results of the Knudsen effusion and Calvet microcalorimetry measurements, respectively. This material is available free of charge via the Internet at <http://pubs.acs.org>.

References and Notes

- (1) Canongia Lopes, J. N.; Cabral do Couto, P.; Minas da Piedade, M. E. *J. Phys. Chem. A* **2006**, *110*, 13850–13856.
- (2) Lousada, C. M.; Pinto, S. S.; Canongia Lopes, J. N.; Piedade, M. F. M.; Diogo, H. P.; Minas da Piedade, M. E. *J. Phys. Chem. A* **2008**, *112*, 2977–2987.
- (3) Cordes, J. F.; Schreiner, S. Z. *Anorg. Chem.* **1959**, *299*, 87–91.
- (4) (a) Baev, A. K.; Demyanchuk, V. V. *Obshch. Prikl. Khim.* **1971**, *6*, 5–72. (b) Baev, A. K.; Demyanchuk, V. V. *Chem. Abstr.* **1970**, *74*, 103799z.

- (5) Chhor, K.; Pommier, C.; Diot, M. *Mol. Cryst. Liq. Cryst.* **1983**, *100*, 193–209.
- (6) Jorgensen, W. L.; Maxwell, D. S.; Tirado-Rives, J. *J. Am. Chem. Soc.* **1996**, *118*, 11225–11236.
- (7) Kaminski, G.; Jorgensen, W. L. *J. Phys. Chem.* **1996**, *100*, 18010–18013.
- (8) Cornell, W. D.; Cieplak, P.; Bayly, C. I.; Gould, I. R.; Merz, K. M.; Ferguson, D. M.; Spellmeyer, D. C.; Fox, T.; Caldwell, J. W.; Kollman, P. A. *J. Am. Chem. Soc.* **1995**, *117*, 5179–5197.
- (9) Parameters obtained from file parm99.dat corresponding to AMBER versions 1999 and 2002.
- (10) Laugier, J.; Bochu, B. *Checkcell* <http://www.ccp14.ac.uk/tutorial/Imgp>.
- (11) Moura Ramos, J. J.; Taveira-Marques, R.; Diogo, H. P. *J. Pharm. Sci.* **2004**, *93*, 1503–1507.
- (12) Hyams, I. J.; Bailey, R. T.; Lippincott, E. R. *Spectrochim. Acta* **1967**, *A23*, 273–284.
- (13) Parker, D. J. *J. Chem. Soc., Dalton Trans.* **1974**, 155–162.
- (14) Todd, L. J.; Wilkinson, J. R. *J. Organomet. Chem.* **1974**, *77*, 1–25.
- (15) Chisholm, M. H.; Godleski, S. *Prog. Inorg. Chem.* **1976**, *20*, 299–436.
- (16) Fitzpatrick, P. J.; le Page, Y.; Sedman, J.; Butler, I. S. *Inorg. Chem.* **1981**, *20*, 2852–2861.
- (17) Allen, F. H. *Acta Crystallogr.* **2002**, *B58*, 380–388.
- (18) Barros, T. M. V. R.; Santos, R. C.; Fernandes, A. C.; Minas da Piedade, M. E. *Thermochim. Acta* **1995**, *269* (270), 51–60.
- (19) Calado, J. C. G.; Dias, A. R.; Minas da Piedade, M. E.; Martinho Simões, J. A. *Rev. Port. Quím.* **1980**, *22*, 53–62.
- (20) Diogo, H. P.; Minas da Piedade, M. E.; Fernandes, A. C.; Martinho Simões, J. A.; Ribeiro da Silva, M. A. V.; Monte, M. J. S. *Thermochim. Acta* **1993**, *228*, 15–22.
- (21) Diogo, H. P.; Minas da Piedade, M. E.; Gonçalves, J. M.; Monte, M. J. S.; Ribeiro da Silva, M. A. V. *Eur. J. Inorg. Chem.* **2001**, *228*, 257–262.
- (22) Kiyobayashi, T.; Minas da Piedade, M. E. *J. Chem. Thermodyn.* **2001**, *33*, 11–21.
- (23) Bernardes, C. E. S.; Santos, L. M. N. B. F.; Minas da Piedade, M. E. *Meas. Sci. Technol.* **2006**, *17*, 1405–1408.
- (24) Frisch, M. J.; Trucks, G. W.; Schlegel, H. B.; Scuseria, G. E.; Robb, M. A.; Cheeseman, J. R.; Montgomery, J. A., Jr.; Vreven, T.; Kudin, K. N.; Burant, J. C.; Millam, J. M.; Iyengar, S. S.; Tomasi, J.; Barone, V.; Mennucci, B.; Cossi, M.; Scalmani, G.; Rega, N.; Petersson, G. A.; Nakatsuji, H.; Hada, M.; Ehara, M.; Toyota, K.; Fukuda, R.; Hasegawa, J.; Ishida, M.; Nakajima, T.; Honda, Y.; Kitao, O.; Nakai, H.; Klene, M.; Li, X.; Knox, J. E.; Hratchian, H. P.; Cross, J. B.; Bakken, V.; Adamo, C.; Jaramillo, J.; Gomperts, R.; Stratmann, R. E.; Yazyev, O.; Austin, A. J.; Cammi, R.; Pomelli, C.; Ochterski, J. W.; Ayala, P. Y.; Morokuma, K.; Voth, G. A.; Salvador, P.; Dannenberg, J. J.; Zakrzewski, V. G.; Dapprich, S.; Daniels, A. D.; Strain, M. C.; Farkas, O.; Malick, D. K.; Rabuck, A. D.; Raghavachari, K.; Foresman, J. B.; Ortiz, J. V.; Cui, Q.; Baboul, A. G.; Clifford, S.; Cioslowski, J.; Stefanov, B. B.; Liu, G.; Liashenko, A.; Piskorz, P.; Komaromi, I.; Martin, R. L.; Fox, D. J.; Keith, T.; Al-Laham, M. A.; Peng, C. Y.; Nanayakkara, A.; Challacombe, M.; Gill, P. M. W.; Johnson, B.; Chen, W.; Wong, M. W.; Gonzalez, C.; Pople, J. A. *Gaussian 03*, revision C.02; Gaussian, Inc.: Wallingford, CT, 2004.
- (25) Becke, A. D. *J. Chem. Phys.* **1993**, *98*, 5648–5652.
- (26) Perdew, J. P.; Wang, Y. *Phys. Rev. B* **1992**, *45*, 13244–13249.
- (27) Leininger, T.; Nicklass, A.; Stoll, H.; Dolg, M.; Schwerdtfeger, P. *J. Chem. Phys.* **1996**, *105*, 1052–1059.
- (28) Dunning, T. H., Jr.; Hay, P. J. In *Modern Theoretical Chemistry*; Schaefer, H. F., III, Ed.; Plenum: New York, 1976; Vol. 3, pp 1–28.
- (29) Breneman, C. M.; Wiberg, K. B. *J. Comput. Chem.* **1990**, *11*, 361–373.
- (30) Smith, W.; Forester, T. R. *The DL POLY Package of Molecular Simulation Routines (v. 2.12)*; The Council for The Central Laboratory of Research Councils; Daresbury Laboratory: Warrington, 1999.
- (31) Halgren, T. A. *J. Am. Chem. Soc.* **1990**, *112*, 4710–4723.
- (32) Santos, L. M. N. B. F.; Canongia Lopes, J. N.; Coutinho, J. A. P.; Esperança, J. M. S. S.; Gomes, L. R.; Marrucho, I. M.; Rebelo, L. P. N. *J. Am. Chem. Soc.* **2007**, *129*, 284–285.
- (33) Wieser, M. E. *Pure Appl. Chem.* **2006**, *78*, 2051–2066.
- (34) Edwards, J. W.; Kington, G. L. *Trans. Farad. Soc.* **1962**, *58*, 1323–1333.
- (35) Andrews, J. T. S.; Westrum, E. F., Jr.; Bjerrum, N. J. *Organomet. Chem.* **1969**, *17*, 293–302.
- (36) Atkins, P. W.; de Paula, J. *Physical Chemistry*, 8th ed.; Oxford University Press: Oxford, 2006; p 754.
- (37) Pascual-Ahuir, J. L.; Silla, E.; Tunon, I. *GEPOL93*; http://server.ccl.net/ccap/software/SOURCES/FORTRAN/molecular_surface/gepol93/.
- (38) Bondi, A. J. *Phys. Chem.* **1964**, *68*, 441–451.
- (39) Denbigh, K. *The Principles of Chemical Equilibrium*, 4th ed.; Cambridge University Press: Cambridge, 1981.
- (40) Korn, G. A.; Korn, T. M. *Mathematical Handbook for Scientists and Engineers*; McGraw-Hill: New York, 1968.
- (41) Irikura, K. K.; Frurip, D. J. *Computational Thermochemistry. Prediction and Estimation of Molecular Thermodynamics*. ACS Symposium Series No. 677; ACS: Washington, 1998.
- (42) Olofsson, G. Assignment of Uncertainties. In *Experimental Chemical Thermodynamics*; Sunner, S.; Månsson, M., Eds.; Pergamon Press: Oxford, 1979; Vol. 1, pp 137–159.

JP805607D